Electronic Supplementary Information

Spatial Control of Cocatalysts and Elimination of Interfacial Defects towards Efficient and Robust CIGS Photocathodes for Solar Water Splitting

Mengxin Chen,[a] Yang Liu,[b] Chengcheng Li,[a] Ang Li,[a] Xiaoxia Chang,[a] Wei Liu,[b] Yun Sun,[b] Tuo Wang[a]* and Jinlong Gong[a]*

[a.] *Key Laboratory for Green Chemical Technology of Ministry of Education, School of Chemical Engineering and Technology, Tianjin University; Collaborative Innovation Center of Chemical Science and Engineering (Tianjin), Tianjin 300072, China*

[b.] *Institute of Photoelectronic Thin Film Devices and Technology and Tianjin Key Laboratory of Thin Film Devices and Technology, Nankai University, Tianjin 300071, China*

* Corresponding authors: jlgong@tju.edu.cn, wangtuo@tju.edu.cn; Fax: +86-22-87401818

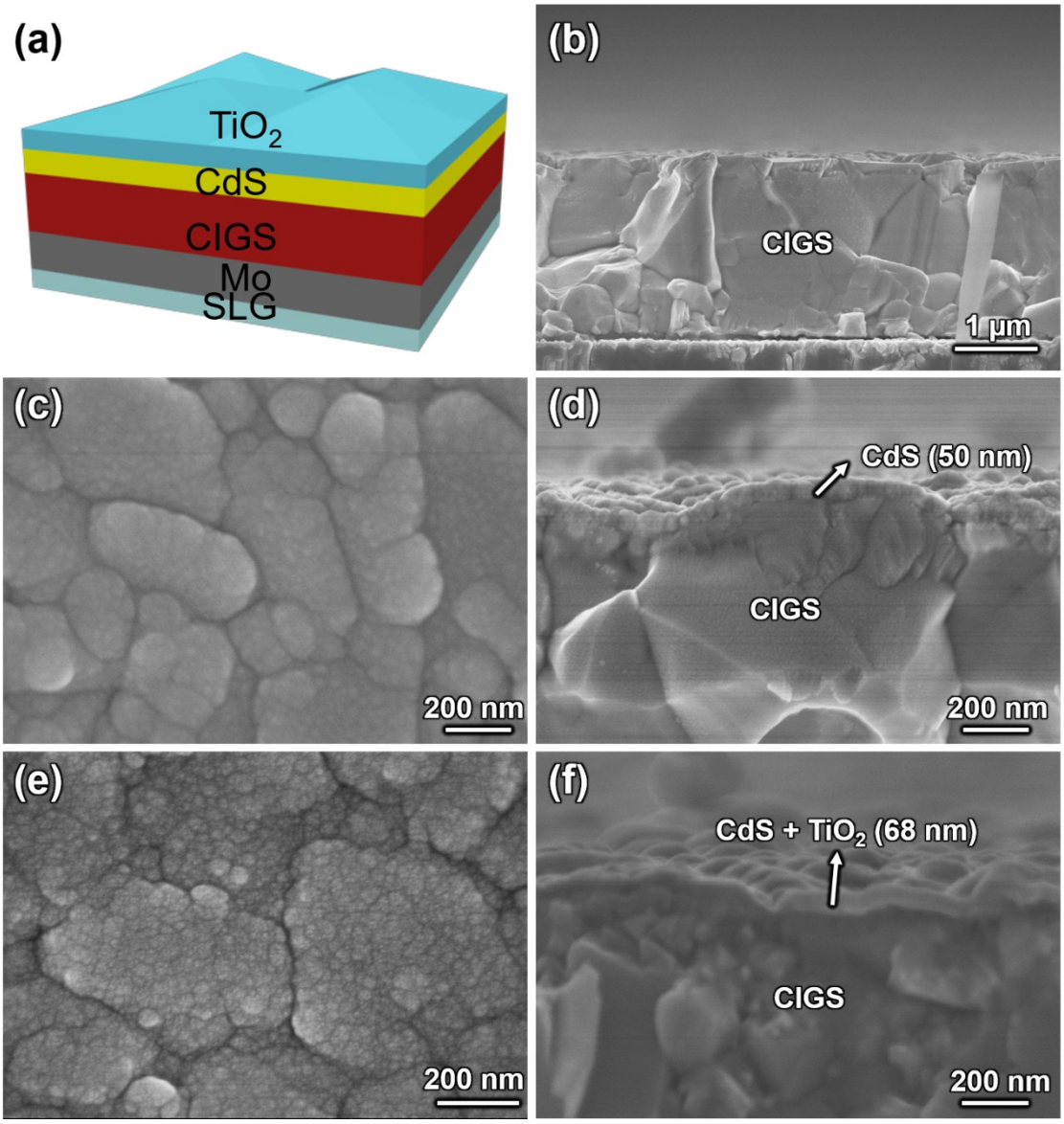

Fig. S1 (a) The schematic of CIGS/CdS/TiO_2 sample, (b) side view SEM image of CIGS, (c, d) top and side view SEM images of CIGS/CdS, (e, f) top and side view SEM images of CIGS/CdS/TiO_2. SLG stands for soda lime glass.

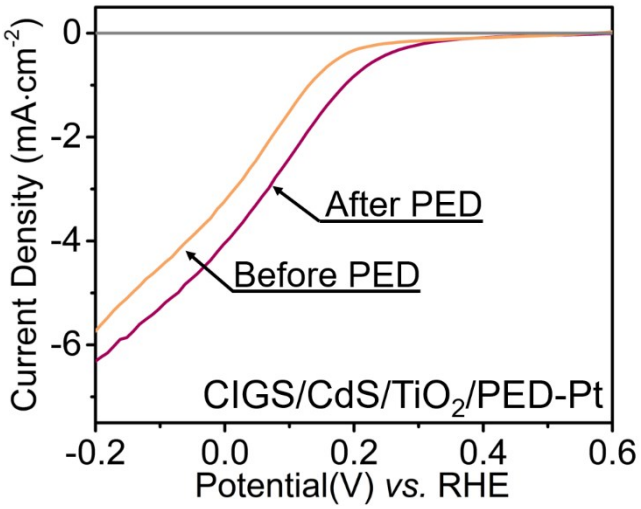

Fig. S2 (a) Current-potential (*J-V*) curves of CIGS/CdS/TiO_2 electrodes loaded with PED-Pt, where the two electrodes are the same samples as in Fig. 1b and d. The curves are measured in 1 M phosphate buffer electrolyte (pH 6.8) under simulated AM 1.5G illumination (100 mW cm^{-2}).

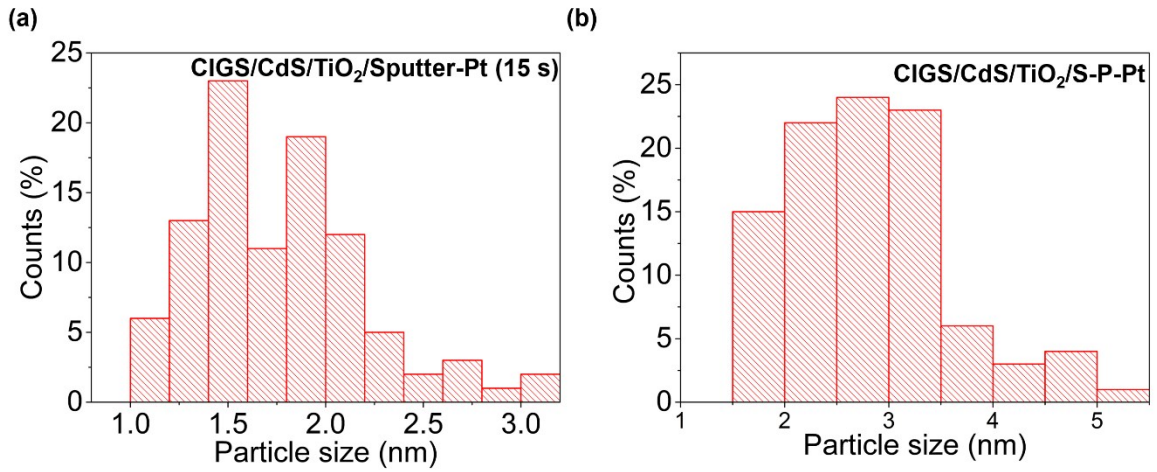

Fig. S3 (a) The corresponding Pt particle size distributions of Sputter-Pt in Fig. 1f and (b) that of S-P-Pt in Fig. 1h, with an average of 1.76 ± 0.05 nm for Sputter-Pt, and 2.86 ± 0.05 nm for S-P-Pt. The size distributions were obtained by counting 100 particles in each sample.

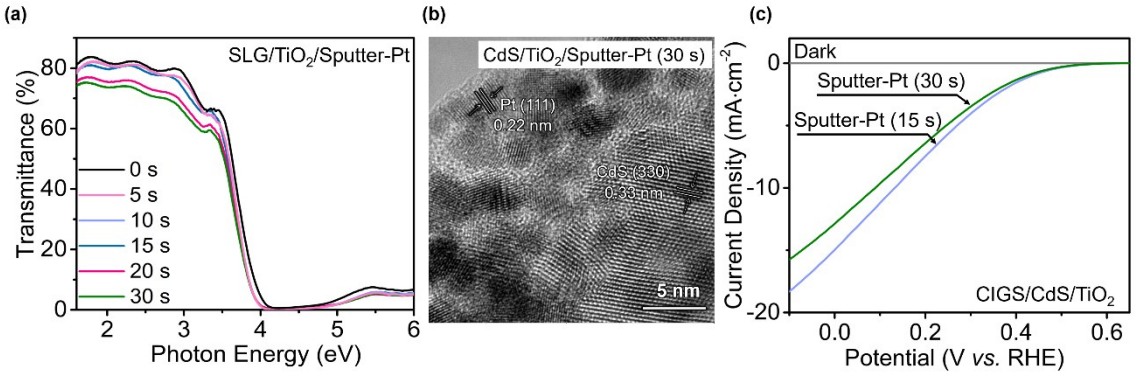

Fig. S4 (a) UV-vis transmission spectra of SLG/TiO_2/Sputter-Pt with different amount of Sputter-Pt. (b) TEM image of CdS/TiO_2/Sputter-Pt, in which the sputter time is 30 s. (c) *J-V* curves of CIGS/CdS/TiO_2 electrodes loaded with different amount of Sputter-Pt. The Pt mass loading of sputter is confirmed by ICP-OES. A sputter time of 15 s is used to deposit 420 ± 5 ng cm^{-2} of Pt and 30 s is used to deposit 1000 ± 10 ng cm^{-2} of Pt.

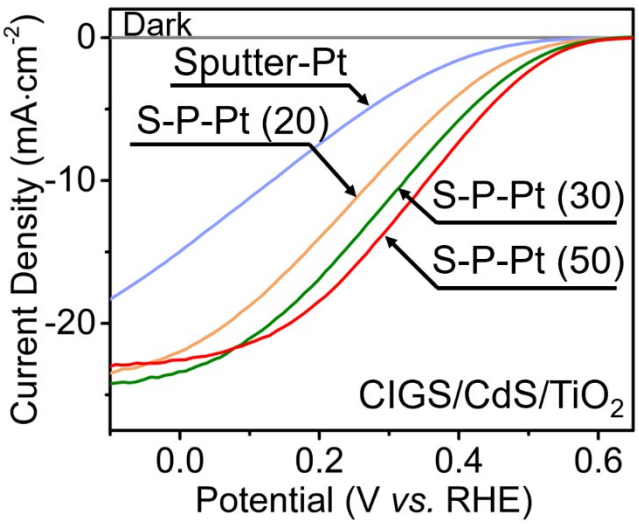

Fig. S5 *J-V* curves of CIGS/CdS/TiO_2 electrodes treated with only Sputtered Pt (blue line) and two-step deposited Pt (yellow, green, and red lines). S-P-Pt (20) refers that electric charge transfer of 20 mC passed through the electrode when Pt NPs are photo-assisted electrodeposited on the CIGS/CdS/TiO_2/Sputter-Pt electrodes.

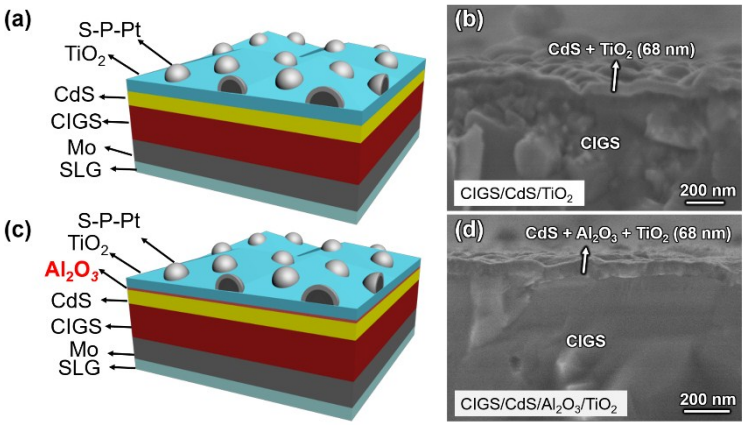

Fig. S6 (a) Photocathode schematic and (b) side view SEM images of CIGS/CdS/TiO_2. (c) Photocathode schematic and (d) side SEM images of CIGS/CdS/Al_2O_3/TiO_2. The ALD cycle numbers for TiO_2 are the both 700 in these two samples, and the corresponding thickness is 18 nm measured by spectroscopic ellipsometer. The Al_2O_3 thickness is 0.5 nm (5 ALD cycles).

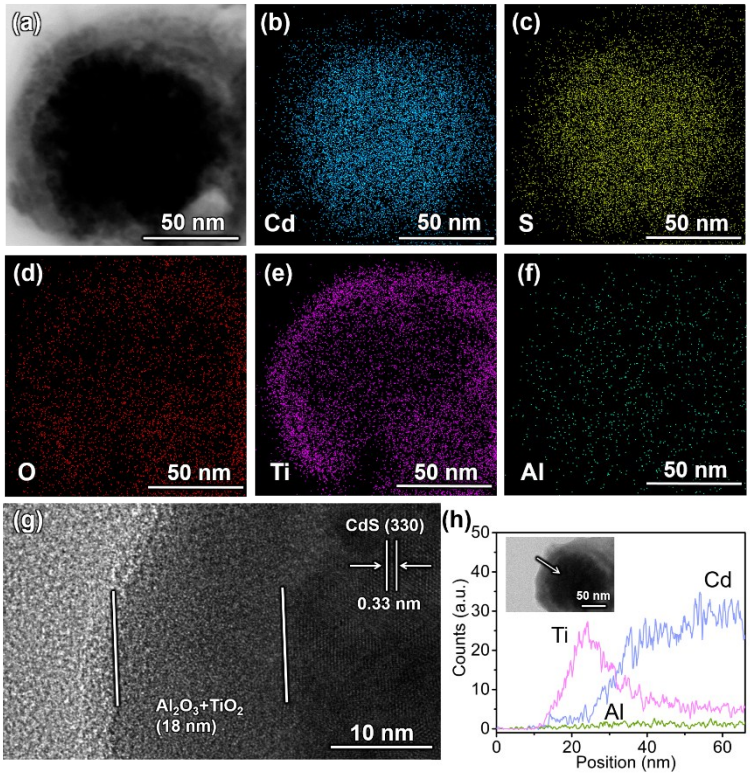

Fig. S7 (a) TEM images, and (b-f) EDS elemental mapping of $CdS/Al_2O_3/TiO_2$ film, in which the thickness of Al_2O_3 is 0.5 nm (5 cycles ALD alumina). (g) TEM images of $CdS/Al_2O_3/TiO_2$ film. (h) EDS compositional line scan as marked in inset.

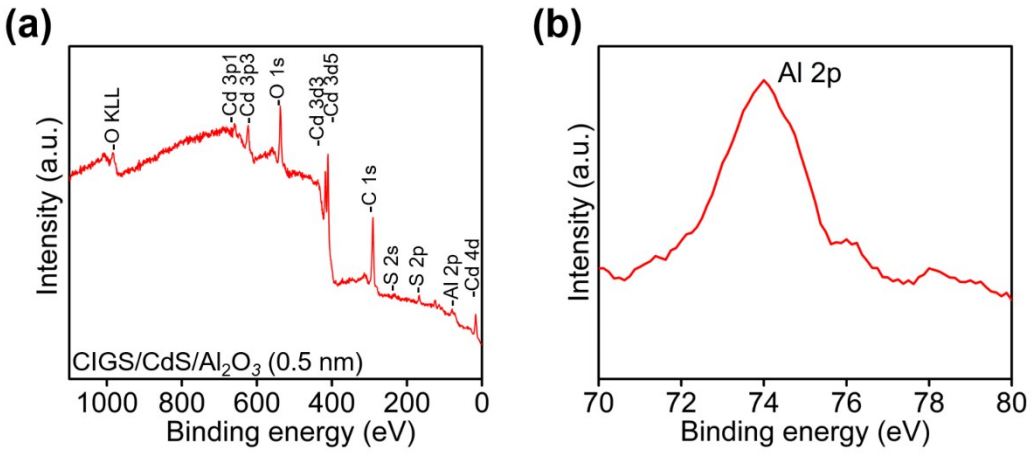

Fig. S8 (a) XPS spectrum for CIGS/CdS junction with 5 cycles (0.5 nm) of Al_2O_3 passivation layer. (b) High-resolution XPS spectrum of the Al 2p of sample in (a).

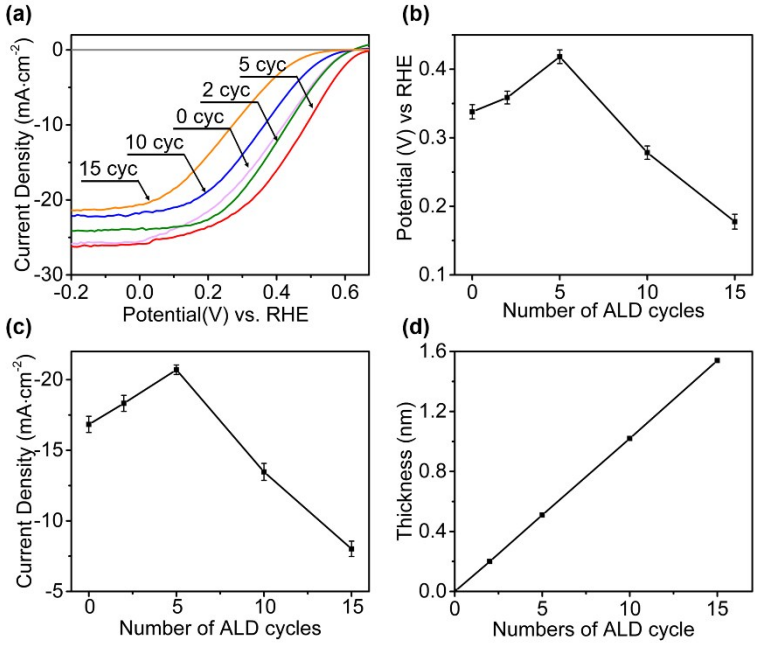

Fig. S9 (a) *J-V* curves of CIGS/CdS/Al_2O_3/TiO_2/S-P-Pt photocathodes with different numbers of (TMA + H_2O) ALD cycles, (b) potentials at 15 mA cm^{-2} for electrodes with various ALD cycles (TMA + H_2O), (c) photocurrents at 0.4 V_{RHE} for electrodes with various ALD cycles (TMA + H_2O). (d) The ALD alumina growth on Si (100) substrate measured by spectroscopic ellipsometer as a function of ALD cycles. The best performance is obtained when the thickness of Al_2O_3 is 0.5 nm, which suppress the deep trap states between CdS and TiO_2 and at the same time, electrons can tunnel through this ultra-thin film.

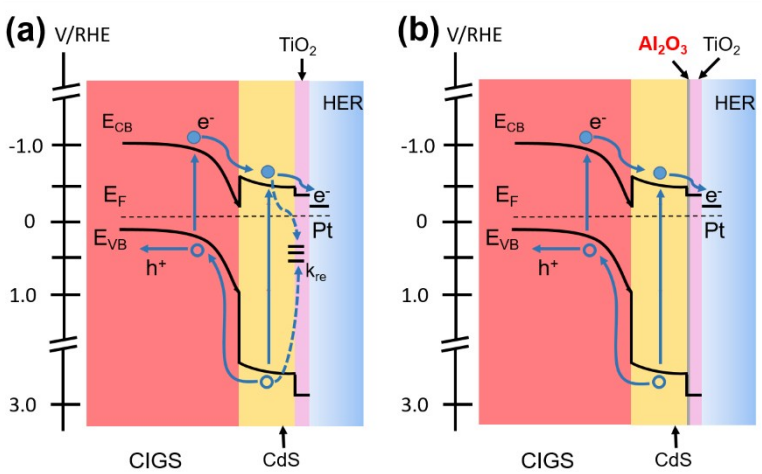

Fig. S10 (a) Electronic band structure of CIGS photocathode without and (b) with an Al_2O_3 passivation layer, indicating the suppression of interfacial recombination for improved electron transfer.

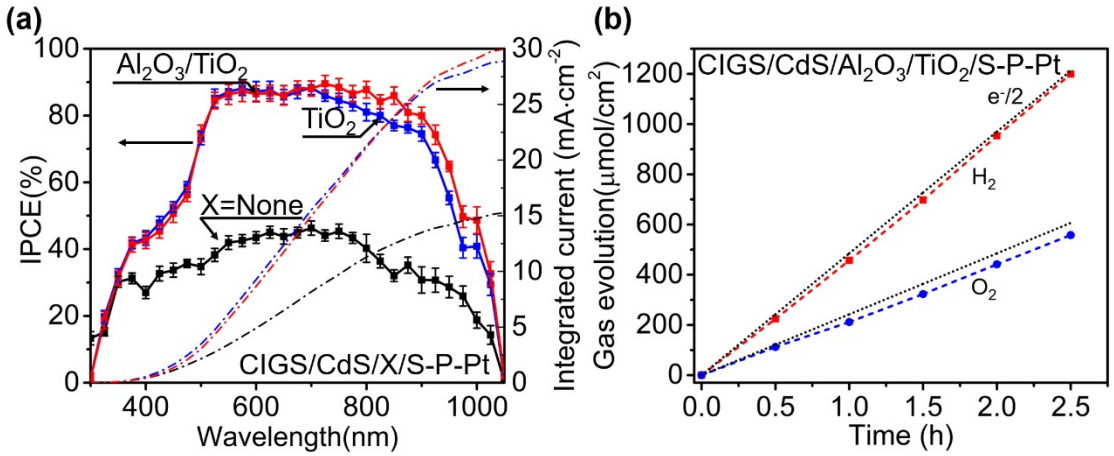

Fig. S11 (a) IPCE of CIGS/CdS/S-P-Pt, CIGS/CdS/TiO_2/S-P-Pt, and CIGS/CdS/Al_2O_3/TiO_2/S-P-Pt photocathodes as a function of wavelength at 0 V_{RHE}. (b) Hydrogen and oxygen evolution for the CIGS/CdS/Al_2O_3/TiO_2/S-P-Pt electrode. The curves (a, b) were measured in 1 M phosphate buffer electrolyte (pH 6.8). The Al_2O_3 thickness in the measurement above is 0.5 nm (5 ALD cycles).

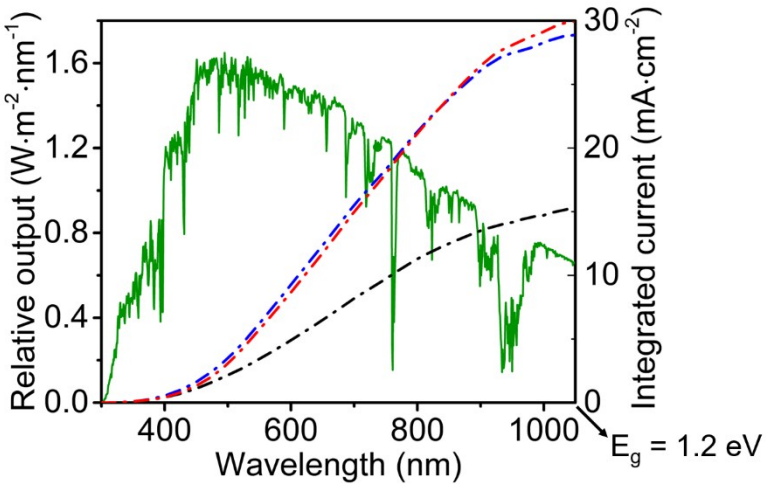

Fig. S12 Details of the wavelengths for standard solar spectrum (ASTM GG173-03) and calculated photocurrents by integrating IPCE over the photon flux of AM 1.5G of the CIGS-based photocathodes in Fig. S11a. The red, blue and black dash lines are corresponding to CIGS/CdS/Al_2O_3/TiO_2/S-P-Pt, CIGS/CdS/TiO_2/S-P-Pt, and CIGS/CdS/S-P-Pt photocathodes. And the wavelength value at the end of x-axis is 1050 nm, which is corresponding to the band gap of CIGS.

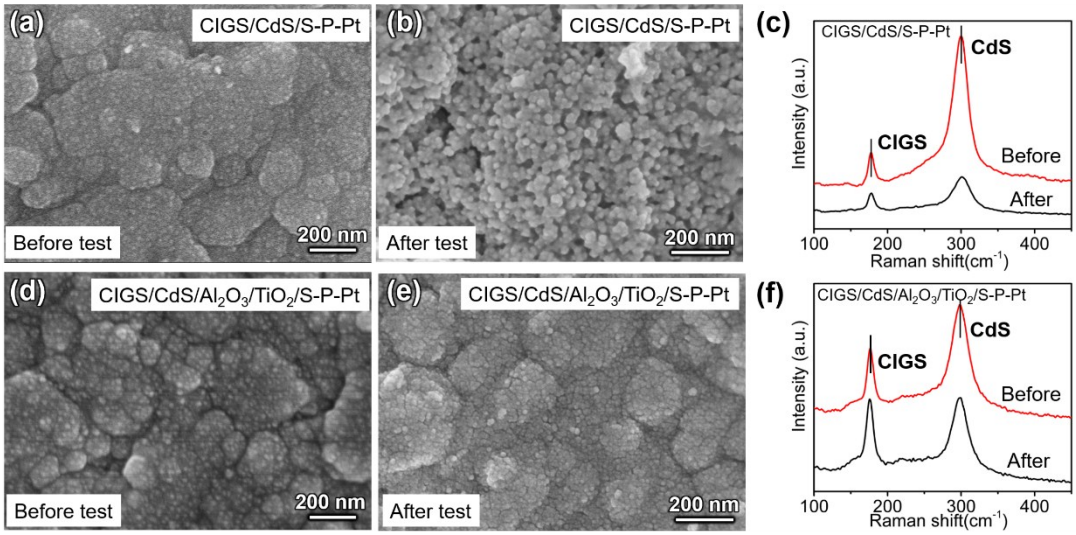

Fig. S13 (a, b) Top view SEM images of CIGS/CdS/S-P-Pt before and after an 8 h durability, and (c) the corresponding Raman spectra of CIGS/CdS/S-P-Pt after the 8 h durability test. (d, e) CIGS/CdS/Al_2O_3/TiO_2/S-P-Pt photocathodes before and after an 8 h durability test, and (f) the corresponding Raman spectra of CIGS/CdS/Al_2O_3/TiO_2/S-P-Pt after the 8 h durability. The durability tests were measured in 1 M phosphate buffer electrolyte (pH 6.8).

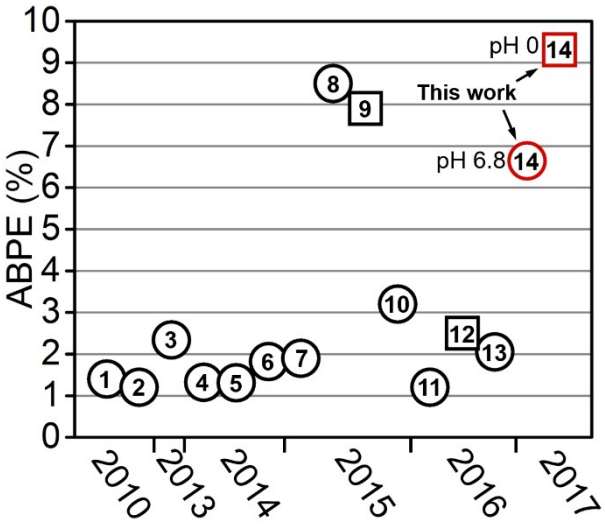

Fig. S14 Chart visualizing data on reported ABPE value of chalcopyrite thin film materials based photocathodes for water reduction. The hollow circles are referred to the work which are measured in near-neutral electrolyte (pH 6~9), and the hollow square are referred to the work which are measured in strong acid electrolyte (pH 0). The sample in black are referred to the reported work and the samples in red are referred to our work, respectively. Details are provided in the **Table S2**.

Table S1 Values of equivalent circuit elements by fitting the experiment data in **Fig. 2b** for the three samples.

Samples	R_b (ohm cm^{-2})	Estimated error (%)	R_{ct} (ohm cm^{-2})	Estimated error (%)	C (F)	Estimated error (%)	Chi-square (%)
CIGS/CdS/TiO_2/Sputter-Pt (30 s)	33.89	0.8313	89.97	0.9231	8.98×10^{-5}	1.2891	0.4860
CIGS/CdS/TiO_2/Sputter-Pt (15 s)	35.55	1.4378	85.22	2.8793	6.7064×10^{-5}	2.3421	0.6986
CIGS/CdS/TiO_2/S-P-Pt	33.69	0.3699	44.95	0.5778	2.8376×10^{-5}	0.7198	0.0153

Table S2 Summary of recent representative reports on chalcopyrite thin film material-based photocathode for hydrogen evolution in **Fig. S14**.

Sample ID	Photocathode	Electrolyte/pH	Reported stability	J at 0 V_{RHE} (mA cm^{-2})	E(onset) (V_{RHE})	ABPE (%)	FF (%)
1[1]	CIGS/CdS/Pt	0.1 M Na_2SO_4/9.5	-	12.0	0.6	1.4	19.4
2[2]	CZTS/CdS/TiO_2/Pt	0.1 M Na_2SO_4/9	-	9.0	0.52	1.2	30.7
3[3]	$CuGaSe_2$/CdS/Pt	0.1 M Na_2SO_4/9.5	25 h	19.0	0.6	2.34	20.5
4[4]	CGSe (Cu:Ga=2)/CdS/Pt	0.1 M Na_2SO_4/9.5	16 h	9.5	0.6	1.32	23.2
5[5]	AgCGSe/CdS/Pt	0.1 M Na_2SO_4/9.5	55 h	8.1	0.7	1.31	23.1
6[6]	$CuInS_2$/CdS/TiO_2/Pt	0.1 M Na_2HPO_4/10	1 h (>420 nm)	14.0	0.65	1.82	20.0
7[7]	AgCGSe/$CuGa_3Se_5$/CdS/Pt	0.1 M Na_2HPO_4/7	20 days (>420 nm)	8.9	0.65	1.9	34.4

8[8]	CIGS/CdS/Ti/Mo/Pt	0.25 M Na_2HPO_4/NaH_2PO_4 /6.8	20 days (25% drop)	30.0	0.59	8.5	47.2
9[9]	CIGS/CdS/i-ZnO/TiO_2/Pt	0.5 M H_2SO_4 /0	1 h(chopped)	34.0	0.6	7.9	38.7
10[10]	CIGS/CdS/ZnO/Pt	0.1 M Na_2SO_4/9	-	32.4	0.6	3.2	16.5
11[11]	CIGS(sulfur)/CdS/TiO_2/Pt	0.1 M Na_2HPO_4/6.1	100 min	5.1	0.65	1.2	36.2
12[12]	CIGS/CdS/i-ZnO/AZO/TiO_2/Pt	0.5 M H_2SO_4 /0.3	1 h (25% drop)	32.0	0.35	2.5	22.3
13[13]	$(ZnSe)_{0.85}(CIGS)_{0.15}$/CdS/Ti/Mo/Pt	1 M Na_2HPO_4/NaH_2PO_4 /6.8	1 h	7.1	0.85	2.05	34.0
14(This work)	CIGS/CdS /Al_2O_3/TiO_2/S-P-Pt	1 M Na_2HPO_4/NaH_2PO_4 /6.8	8 h (4.5% drop)	26.2	0.63	6.6	40.5
		1 M $HClO_4$/0	2 h (6% drop)	27.2	0.63	9.3	54.7

Table S3 Summary of recent representative reports on various thin film material-based photocathodes for hydrogen evolution.

Photocathode	Electrolyte/pH	Reported stability	J at 0 V_{RHE} (mA cm^{-2})	E(onset) (V_{RHE})	ABPE (%)	FF (%)
CZTS/CdS/In_2S_3/Pt[14]	0.2 M Na_2HPO_4/NaH_2PO_4 /6.5	3 h (0% drop)	8.7	0.57	1.63	32.1
Ge-CZTS/CdS/In_2S_3/Pt[15]	0.2 M Na_2HPO_4/NaH_2PO_4 /6.5	N.A.	11.1	0.6	1.7	25.5
a-Si (p-i-n)/TiO_2/Pt[16]	0.5 M $C_8H_5KO_4$/4	12 h (5% drop)	11.6	0.93	6.0	55.5
CdTe/CdS/Pt[17]	0.5 M KH_2PO_4/8	11 h (37% drop)	8.4	0.6	0.9	17.8
Au/Cu/CdTe/CdS/Pt[18]	1 M KH_2PO_4/8	70 min (0% drop)	22.0	0.6	3.7	28.1
CIGS/CdS /Al_2O_3/TiO_2/S-P-Pt (our work)	1 M Na_2HPO_4/NaH_2PO_4 /6.8	8 h (4.5% drop)	26.2	0.63	6.6	40.5
	1 M $HClO_4$/0	2 h (6% drop)	27.2	0.63	9.3	54.7

Supplement References:

1. D. Yokoyama, T. Minegishi, K. Maeda, M. Katayama, J. Kubota, A. Yamada, M. Konagai and K. Domen, *Electrochem. Commun.*, 2010, **12**, 851-853.
2. Y. Daisuke, M. Tsutomu, J. Kazuo, H. Takashi, M. Guijun, K. Masao, K. Jun, K. Hironori and D. Kazunari, *Appl. Phys. Express*, 2010, **3**, 101202.
3. M. Moriya, T. Minegishi, H. Kumagai, M. Katayama, J. Kubota and K. Domen, *J. Am. Chem. Soc.*, 2013, **135**, 3733-3735.
4. H. Kumagai, T. Minegishi, Y. Moriya, J. Kubota and K. Domen, *J. Phys. Chem. C*, 2014, **118**, 16386-16392.
5. L. Zhang, T. Minegishi, J. Kubota and K. Domen, *Phys. Chem. Chem. Phys.*, 2014, **16**, 6167-6174.
6. J. Zhao, T. Minegishi, L. Zhang, M. Zhong, Gunawan, M. Nakabayashi, G. Ma, T. Hisatomi, M. Katayama, S. Ikeda, N. Shibata, T. Yamada and K. Domen, *Angew. Chem. Int. Ed.*, 2014, **53**, 11808-11812.
7. L. Zhang, T. Minegishi, M. Nakabayashi, Y. Suzuki, K. Seki, N. Shibata, J. Kubota and K. Domen, *Chem. Sci.*, 2015, **6**, 894-901.
8. H. Kumagai, T. Minegishi, N. Sato, T. Yamada, J. Kubota and K. Domen, *J. Mater. Chem. A*, 2015, **3**, 8300-8307.
9. J. Luo, Z. Li, S. Nishiwaki, M. Schreier, M. T. Mayer, P. Cendula, Y. H. Lee, K. Fu, A. Cao, M. K. Nazeeruddin, Y. E. Romanyuk, S. Buecheler, S. D. Tilley, L. H. Wong, A. N. Tiwari and M. Grätzel, *Adv. Energy Mater.*, 2015, **5**, 1501520.
10. M. G. Mali, H. Yoon, B. N. Joshi, H. Park, S. S. Al-Deyab, D. C. Lim, S. Ahn, C. Nervi and S. S. Yoon, *ACS Appl. Mater. Interfaces*, 2015, **7**, 21619-21625.
11. N. Guijarro, M. S. Prévot, X. Yu, X. A. Jeanbourquin, P. Bornoz, W. Bourée, M. Johnson, F. Le Formal and K. Sivula, *Adv. Energy Mater.*, 2016, **6**, 1501949.
12. C. Ros, T. Andreu, S. Giraldo, Y. Sánchez and J. R. Morante, *Sol. Energy Mater. Sol. Cells*, 2016, **158**, 184-188.
13. H. Kaneko, T. Minegishi, M. Nakabayashi, N. Shibata, Y. Kuang, T. Yamada and K. Domen, *Adv. Funct. Mater.*, 2016, **26**, 4570-4577.
14. F. Jiang, Gunawan, T. Harada, Y. Kuang, T. Minegishi, K. Domen and S. Ikeda, *J. Am. Chem. Soc.*, 2015, **137**, 13691-13697.
15. X. Wen, W. Luo, Z. Guan, W. Huang and Z. Zou, *Nano Energy*, 2017, **41**, 18-26.
16. Y. Lin, C. Battaglia, M. Boccard, M. Hettick, Z. Yu, C. Ballif, J. W. Ager and A. Javey, *Nano Lett.*, 2013, **13**, 5615-5618.
17. J. Su, T. Minegishi, M. Katayama and K. Domen, *J. Mater. Chem. A*, 2017, **5**, 4486-4492.
18. J. Su, T. Minegishi and K. Domen, *J. Mater. Chem. A*, 2017, **5**, 13154-13160.